Energy 351 (2026) 140773

Contents lists available at ScienceDirect

Energy

journal homepage: www.elsevier.com/locate/energy

Design and thermodynamic assessment of a sustainable waste to energy system for multiple useful outputs

Ayse Sinem Meke [a,*], Ibrahim Dincer [a], Ali Khalvati [b]

[a] Clean Energy Research Laboratory (CERL), Faculty of Engineering and Applied Science, Ontario Tech. University, 2000 Simcoe Street North, Oshawa, Ontario, L1G 0C5, Canada

[b] Viona Consulting Inc., Agro-Environmental Innovation and Technology, Research and Development Company, Thornhill, Ontario, L3T 0C6, Canada

ARTICLE INFO

Keywords:
Efficiency
Energy
Exergy
Hydrogen
Waste
Wastewater
Freshwater
Dark fermentation

ABSTRACT

This study includes the development and thermodynamic performance assessment of a new sustainable multi-generation system, with the Woodward Avenue Wastewater Treatment Plant in Hamilton, Ontario, Canada selected as a potential implementation site. The integrated configuration covers sludge incineration, dark fermentation (DF), hydrochar production via hydrothermal carbonization (HTC), organic Rankine cycle (ORC), multi-effect desalination (MED), and a wind farm subsystem to simultaneously produce hydrogen, hydrochar, freshwater, and electricity from wastewater sludge and renewable energy sources. The proposed system achieved an overall energy efficiency of 48% and an exergy efficiency of 42%, demonstrating strong thermodynamic balance and effective heat recovery. The present system is potentially designed to produce approximately 13,950 kg of hydrogen, 1490 tonnes of hydrochar, 35,500 m^3 of freshwater, and 160 MWh of electricity annually. The results confirm that the integrated system provides an efficient and sustainable approach for waste-to-energy conversion and resource recovery, enabling simultaneous production of clean energy and valuable by-products. An exergoeconomic analysis further highlights the dominant cost drivers and confirms the economic feasibility of the proposed integrated system. The proposed configuration represents a feasible pathway toward low-carbon, circular, and energy-positive wastewater treatment infrastructure.

1. Introduction

The rapid increase in global energy demand and the use of fossil fuels as the primary energy source for many years have led to the emergence of serious environmental problems around the world [1]. Carbon dioxide (CO_2), nitrogen oxides (NO_x), and other harmful gases released from the combustion of fossil fuels accumulate in the atmosphere, strengthening the greenhouse effect and accelerating climate change [2]. This situation causes not only environmental challenges, but also economic and social crises [3]. Therefore, replacing existing energy systems with sustainable alternatives has become essential for both energy security and environmental protection [4].

In this context, the shift towards renewable energy sources has gained significant momentum in recent years [5]. Solar energy generates electricity and heat through direct solar radiation, while geothermal energy uses underground heat to provide continuous energy production [6]. Biomass energy utilizes agricultural and organic waste as fuel, while hydroelectric energy provides a reliable energy flow by harnessing the potential energy of water [7]. Furthermore, marine-based systems such as wave and tidal energy are also at the forefront of next-generation energy conversion technologies [8].

Among these renewable resources, wind energy has become one of the fastest-growing energy sources, due to its low carbon emissions, broad applicability, and technological maturity [9]. Wind turbines can operate with high efficiency and provide stable electricity production, especially in coastal areas or high altitude regions [10]. Furthermore, a sustainable energy future is possible not only through renewable generation but also through waste management, resource recovery, and the integration of multiple production systems [11]. Temiz et al. [12] developed an integrated solar and wind energy system that completely met the electricity, heat, and cooling needs of a community of 65,000 people. The system's sustainability was ensured through the integration of energy storage and multiple outputs (electricity, heat, cooling, freshwater, and hydrogen). Annually, 363,344.7 MWh of electricity,

This article is part of a special issue entitled: SEEP2025 - Invitation Only published in Energy.

* Corresponding author.
E-mail address: ayse.meke@ontariotechu.net (A.S. Meke).

https://doi.org/10.1016/j.energy.2026.140773
Received 5 November 2025; Received in revised form 17 December 2025; Accepted 15 March 2026
Available online 17 March 2026

544,468.2 MWh of heat, 192,112.7 MWh of cooling, 24,142 kt of freshwater, and 38,843 tons of hydrogen were produced. The system achieved an average energy efficiency of 37.69% and exergy efficiency of 28.27%.

Sewage sludge represents an environmentally problematic but potentially valuable energy resource [13]. Wastewater treatment plants worldwide produce millions of tons of sludge annually, and direct disposal of this sludge is costly and environmentally risky [14]. However, because sludge contains high levels of organic matter, carbon, nitrogen, and minerals, it can be converted into energy and useful products through appropriate processes [15]. This conversion can be achieved through methods such as incineration [16], anaerobic digestion [17], dark fermentation (DF) [18], and hydrothermal carbonization (HTC) [19]. For example, dark fermentation is an environmentally friendly biological process that produces hydrogen (H_2) from organic waste with the help of microorganisms [20]. Because this method operates at low temperatures, it requires less energy and produces clean fuel without the need for fossil fuels [21]. Sludge incineration, on the other hand, reduces waste volume through high-temperature combustion and generates thermal energy [22]. This energy can then be used in other components of the system.

Gao et al. [23] developed a multigeneration system by integrating sludge hydrothermal carbonization (HTC) with a small modular nuclear reactor. The system produced 188.81 MW of net power, 62.88 kg/s of freshwater, and achieved a total efficiency of 34.34%, an electrical efficiency of 30.04%, and a sludge-to-electricity conversion efficiency of 16.82%. The exergy efficiency of the hydrothermal carbonization (HTC) process was 37.08%, and the system payback period was 6.44 years. Similarly, Aydin et al. [24] conducted a comparative study of hydrogen production methods from wastewater. Eight different methods were evaluated including dark fermentation, microbial electrolysis, and photofermentation were determined to be the most economically viable technologies. Microbial electrolysis was identified as the most environmentally friendly method with the lowest global warming potential. Furthermore, microbial electrolysis demonstrated the highest performance with 68% energy and 64.7% exergy efficiency.

Waste heat recovery is critical for improving the efficiency of such thermochemical and biological processes [25]. The organic Rankine cycle (ORC) generates electrical energy by utilizing low- to medium-temperature waste heat [26]. This maximizes energy recovery and increases the overall efficiency of the system [27]. Abdolalipouradl et al. [28] proposed an innovative multiple generation system based on a biogas-fueled gas turbine (BFGT). The system consists of a biogas-fueled gas turbine (BFGT), a proton exchange membrane fuel cell (PEMFC), an reverse osmosis (RO) desalination unit, an organic Rankine cycle (ORC), and a domestic water heater for electricity, hydrogen, freshwater, and heat production. Thermodynamic and exergoeconomic analyses revealed that the system achieved a thermal efficiency of 62.45% and an exergy efficiency of 32.52%, with an environmental penalty of $1.93/h and a power specific cost of $28.98/GJ.

In this study, a fully integrated multigeneration waste-to-energy system tailored to the conditions of Hamilton, Ontario, Canada, is proposed and thermodynamically evaluated. Unlike many existing multigeneration systems in the literature that focus on a limited combination of technologies or treat biological, thermochemical, and renewable subsystems in isolation, the proposed configuration integrates wind energy, sludge incineration, dark fermentation (DF), hydrothermal carbonization (HTC), an organic Rankine cycle (ORC), and multi-effect desalination (MED) within a single, integrated system boundary.

The primary novelty of this work lies in treating wastewater treatment sludge not only as an energy feedstock but also as a carbon and resource management medium, achieved through the coordinated integration of biological, thermochemical, and renewable pathways using cascaded heat and material integration rather than simple parallel coupling of subsystems. High-temperature flue gas from sludge incineration is directly utilized to drive the organic Rankine cycle (ORC) for electricity generation, while the residual heat from the ORC condenser is strategically recovered to support biological hydrogen production via dark fermentation (DF) and freshwater production through desalination. In parallel, hydrothermal carbonization (HTC) converts a fraction of the sludge into hydrochar, enabling solid carbon retention and material valorization, which is rarely addressed in comparable multigeneration waste-to-energy studies.

Furthermore, the proposed system advances current knowledge by explicitly linking waste-to-energy conversion with carbon management, hydrogen generation, and freshwater recovery within a unified system framework. Hydrochar is treated as a controllable carbon-rich intermediate rather than a byproduct, and the overall heat integration strategy is designed to minimize exergy destruction across biological and thermochemical stages. The inclusion of wind energy as an internal power supply further differentiates this configuration by reducing external grid dependency and enabling a more resilient and self-sustainedoperation.

Overall, this study contributes to the multigeneration energy systems literature by demonstrating how conventional wastewater treatment plants can be transformed into integrated, energy-positive, and low-carbon infrastructure through coordinated heat, material and power integration. By simultaneously producing electricity, hydrogen, hydrochar, and freshwater within a closed-loop and thermodynamically optimized framework, the proposed configuration extends beyond conventional waste-to-energy systems and offers a novel and generalizable pathway for sustainable, circular wastewater-based energy and resource recovery systems.

2. System description

This study covers an integrated wastewater sludge management and energy recovery system potentially proposed for installation at the Woodward Avenue Wastewater Treatment Plant in Hamilton, Ontario. The system aims to process of sludge generated from wastewater treatment plants in an environmentally sustainable manner and convert the thermal energy generated in this process into useful outputs such as electricity, hydrogen, freshwater, and fuel (e.g., hydrochar and hydrogen). The system consists of five main subsystems: (i) sludge incineration plant, (ii) organic Rankine cycle (ORC), (iii) dark fermentation (DF) plant, (iv) hydrochar production unit (HTC), and (v) multi-effect desalination (MED) plant. These subsystems are interconnected through heat and mass integration, with the overall goal of increasing energy efficiency and achieving a zero-waste approach. Schematic representation of the designed system and simulation of the hydrochar process is given in Fig. 1.

2.1. Sludge incineration subsystem

At the wastewater treatment plant, primary sludge exiting the primary sedimentation tanks is first dewatered in a mechanical dehydrator and divided on a mass basis, with 60% directed to incineration, 25% to dark fermentation (DF), and 15% to hydrothermal carbonization (HTC), reflecting typical allocation strategies reported for integrated wastewater-based energy systems. This dewatered process increases the solids content of the sludge while maintaining a constant temperature (293 K, 101 kPa). The dryer then reduces the moisture content and heats the sludge to approximately 350 K. The dried sludge is converted into thermal energy by incineration in an incinerator operating at a temperature between 800 and 1000 °C (1073-1273 K). This process produces hot flue gas (approximately 1173 K, 101 kPa). The flue gas is directed directly to the organic Rankine cycle (ORC) evaporator to be utilized as a high-temperature heat source. After heat recovery, the gas generated after incineration is passed through electrostatic precipitators and wet scrubbers to remove dust and acidic components. Finally, it is released into the atmosphere via the stack. Solid combustion products are removed as ash. The main output of this subsystem is thermal energy

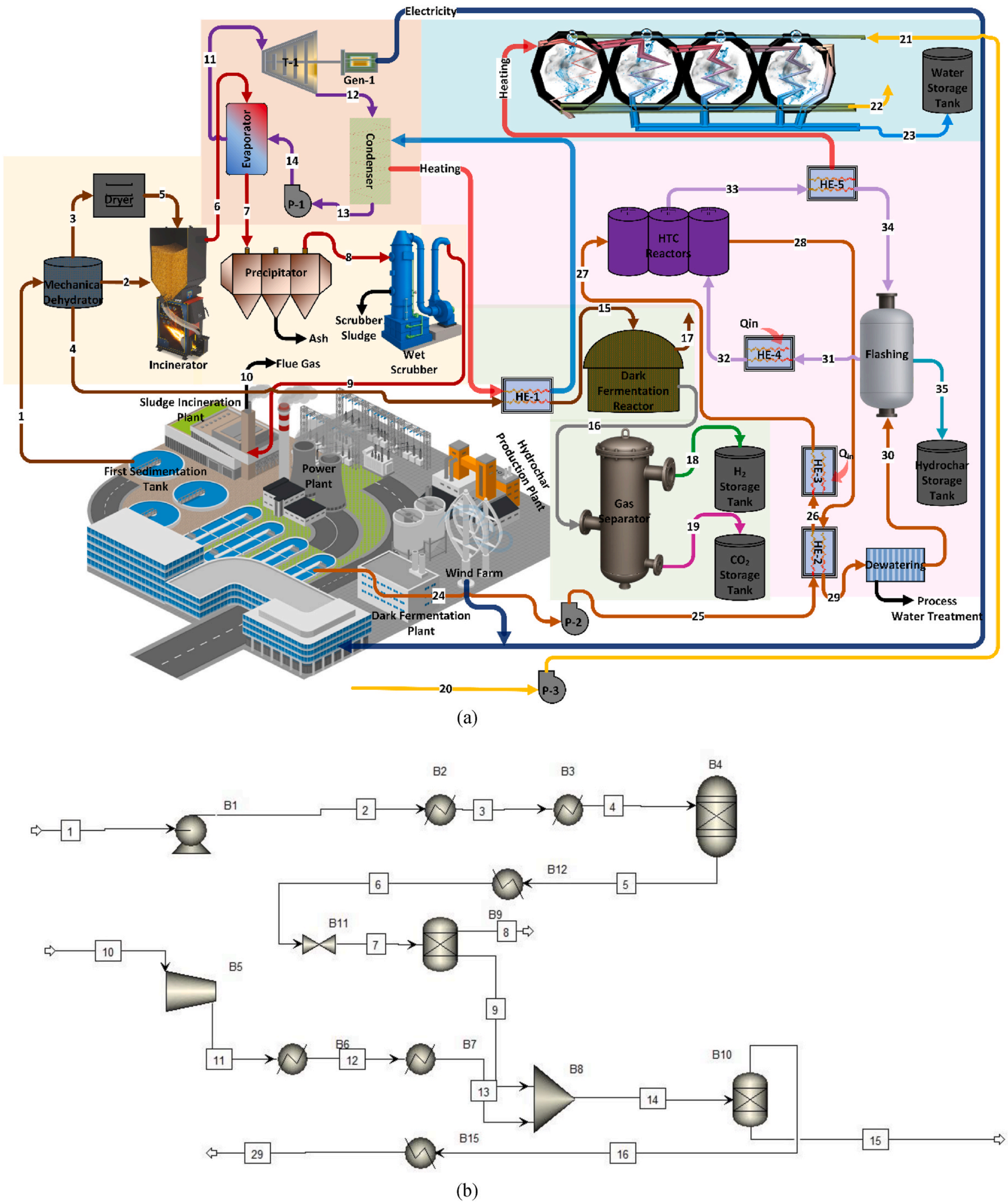

Fig. 1. Schematic illustrations of (a) the proposed system and (b) the Aspen Plus simulation of the hydrochar unit.

(hot flue gas), which also constitutes the main energy source for the organic Rankine cycle (ORC) cycle and heat integration.

2.2. *Organic Rankine Cycle (ORC) subsystem*

The hot flue gas exiting the sludge incineration unit enters the evaporator section of the organic Rankine cycle (ORC) system, converting toluene (the organic working fluid) into superheated vapor. At the evaporator exit, the fluid is at approximately 573 K and 1500 kPa. The vapor passes through a turbine with an isentropic efficiency of 80%, converting it into mechanical energy and then into electrical energy via the generator. The fluid at the turbine exit (approximately 460 K, 120 kPa) is cooled in the condenser, liquefied, and returned to the evaporator by a pump. On the flue gas side, the temperature of the gas exiting the evaporator drops to around 200 °C (473 K) and is then directed to the flue treatment unit. This allows electricity generation from the waste heat generated by the incineration process. By integrating the organic Rankine cycle (ORC) system, the energy recovery efficiency of the wastewater sludge incineration process is significantly increased.

2.3. *Dark fermentation (DF) subsystem*

The dark fermentation (DF) subsystem is a biochemical unit that utilizes a portion of the mechanically dewatered sludge in a wastewater treatment plant for biohydrogen production. A certain percentage of the sludge exiting the mechanical dehydrator is sent directly to the sludge incineration unit as fuel, while the remaining portion is fed to the dark fermentation reactors. This approach aims to increase overall energy efficiency by integrating both biological and thermochemical energy recovery processes into the integrated system. The sludge fed to the system is initially at ambient conditions (approximately 293 K and 101 kPa). To reach the appropriate temperature for fermentation, the sludge is passed through a heat exchanger. The energy required for this heat exchanger is provided by waste heat recovered from the condenser unit in the organic Rankine cycle (ORC) cycle. This integration ensures energy sustainability of the system without the need for external heat input. Dark fermentation is assumed to operate under mesophilic conditions (37 °C, atmospheric pressure) with a hydrogen yield of 80-100 L H_2 kg^{-1} VS, which is representative of sludge-based biological conversion under steady-state operation. The heated sludge is fed to the dark fermentation reactors operating under anaerobic conditions. Reactors break down organic compounds using mixed microorganism consortia operating in an oxygen-free environment. During this process, organic matter, particularly carbohydrates, is biochemically converted, releasing hydrogen (H_2) and carbon dioxide (CO_2) gases. The resulting gas mixture is directed to a gas separation unit at the reactor outlet. This unit separates hydrogen (H_2) and carbon dioxide (CO_2) into separate streams using physical or membrane-based separation methods. Hydrogen gas can be stored as the system's energy carrier or fed directly to the gas turbine, while the carbon dioxide gas stream can be used in chemical conversion or carbon capture processes. The fermented sludge exiting the reactor is returned to the incineration unit as a semi-solid waste with reduced organic content. This completes the system's material cycle and achieves biochemical and thermochemical integration between the dark fermentation (DF) section and the sludge incineration section. This structure enables maximum energy recovery from the wastewater sludge, increasing the overall system efficiency.

2.4. Multi-effect desalination (MED) subsystem

The multi-effect desalination (MED) subsystem constitutes the water recovery unit of the integrated plant and is the thermally integrated part of the process. In this system, lake water is converted into freshwater through a multi-effect evaporation process based on the principle of cascade evaporation. The primary heat input to the multi-effect desalination (MED) unit is low-temperature waste heat recovered from the hydrothermal carbonization (HTC) section of the system. This heat, typically in the range of 80-120 °C (353-393 K), provides the energy required for evaporation in the first effect of the multi-effect desalination (MED) unit. During the hydrochar production process, hot process water and steam from the hydrothermal carbonization (HTC) reactors operating at high pressure and temperature are directed to the multi-effect desalination (MED) unit as a heat source after partially losing their energy in the heat exchanger (HE-5). Thanks to this integrated structure, the waste heat generated from the hydrothermal carbonization (HTC) reactors is directly utilized, significantly reducing the system's total energy consumption. The multi-effect desalination (MED) system uses this heat to vaporize a portion of the seawater in the first effect. The heat generated by the condensation of evaporated water is used to heat the second effect, and this process is repeated across multiple effects. At each stage, the pressure is reduced, allowing the water to boil at lower temperatures. Thus, multiple evaporation-condensation cycles occur with the same amount of heat energy. The condensate generated in each effect is collected as high-purity freshwater, while the residual flow, which has increased salinity, is removed from the system as brine. The resulting freshwater is reused to meet the plant's process water needs or for local use. This subsystem utilizes the waste heat of the hydrothermal carbonization (HTC) unit to provide both water treatment and resource recovery. Thus, energy recovery and water production are combined, resulting in a closed-loop, integrated system for environmental sustainability.

2.5. Hydrochar production subsystem

The hydrochar production process involves processing sewage sludge from a wastewater treatment plant under high temperature and pressure in a hydrothermal carbonization (HTC) reactor. Throughout the process, the sludge is heated and pressurized, resulting in solid, liquid, and gaseous phases. The wastewater sludge is first pressurized to approximately 20 bar by a pump (P-2) and then passed through two-stage heat exchangers (HE-2 and HE-3), raising its temperature from 298 K to approximately 453 K. This process ensures thermal conditioning of the sludge before entering the reactor. Heat is supplied to the HTC reactor by hot air circulating in a closed loop. This air is heated in the heat exchanger (HE-5) and sent to the reactor, where it transfers its heat to the sludge. Thus, the sludge undergoes a hydrothermal reaction at approximately 20 bar pressure and 453-493 K. As a result of the chemical transformations that occur in the HTC reactor, most of the organic components are degraded, producing hydrochar, a hydrocarbon-based solid product, water (process water), and a small amount of gaseous phase (such as CO_2 and CH_4). The hot sludge mixture (slurry) exiting the reactor is cooled in the HE-2 for heat recovery and then sent to the dewatering unit. During the dewatering phase, mechanical separation takes place; the solid phase (hydrochar) in the slurry is separated from the liquid. The solid phase contains approximately 80% hydrochar, while the liquid phase is removed from the system as process water or processed for recycling. The aim of this process is to convert the organic compounds in the wastewater sludge into an energy-dense, carbon-rich solid product. For the thermodynamic modeling of the system, the hydrothermal carbonization (HTC) process is assumed to operate at a representative reaction temperature of 220 °C (493 K) and a pressure of 2 MPa, consistent with typical sludge-based hydrothermal carbonization (HTC) applications. Under these conditions, a hydrochar yield of approximately 55-60% on a dry mass basis is assumed, with the remaining fraction forming the liquid process stream and a minor gaseous phase. This reduces the sludge's disposal burden and allows the hydrochar to be reused for energy production, soil amendments, or as a carbon storage material.

2.6. Wind power subsystem

The wind energy subsystem constitutes the renewable energy component of the integrated facility and aims to meet a significant portion of the system's electricity needs. This subsystem includes 50 vertical-axis wind turbines, and a detailed energy production analysis was conducted using the System Advisor Model (SAM) software. Each turbine was selected for high performance in urban areas where low and variable wind speeds prevail. Vertical-axis turbines were chosen for this system because they have low noise levels, stable operation even in turbulent flows, and are suitable for installation in smaller spaces. These features offer significant advantages for wind energy integration in industrial sites such as the Woodward Avenue Wastewater Treatment Plant. The SAM model was used to calculate the annual energy production potential of the turbines using typical meteorological data for the Hamilton area. An average wind speed was assumed to be 6-7 m/s. The model determined each turbine's nominal power output as 1 kW, a rotor diameter of 2.4 m, and a hub height of 80 m. Table 1 presents the key technical specifications and operating parameters of the wind turbines adopted in the wind farm simulation.

The generated electrical energy is fed directly into the facility's general power grid. This energy is used to meet the electrical needs of auxiliary equipment, particularly the dark fermentation (DF) unit, HTC reactor pumps, and multi-effect desalination (MED) unit. In the event of excess energy production, energy can be transferred to the grid or temporarily stored in energy storage systems. This subsystem reduces the integrated facility's fossil fuel dependency and contributes to the

Table 1
Technical specifications and operating conditions of the wind turbines used in the wind farm model.

Parameter	Value
Rated output	1 kW
Rotor diameter	2.4 m
Hub height	80 m
Shear coefficient	0.15
Maximum coefficient of power (Cp)	0.25
Maximum tip speed	50 m/s
Maximum tip speed ratio	6
Cut-in wind speed	2 m/s
Cut-out wind speed	20 m/s

system's overall energy sustainability and carbon neutrality goals. Thanks to the modular structure of the vertical-axis wind turbines, the system can be scaled in future periods, reducing both environmental impact and increasing the facility's renewable energy share. This integrated system enables sustainable resource recovery by connecting energy, water, and waste cycles. Thermochemical, biochemical, and renewable energy subsystems work together to increase energy efficiency while minimizing environmental impact.

The selection of the Hamilton, Ontario, was based on site-specific environmental conditions that strongly support the integration of renewable energy and resource recovery subsystems. Hamilton is characterized by a moderate and consistent wind regime, with average wind speeds typically reported in the range of 6-7 m/s, particularly along the Lake Ontario shoreline. This wind profile is well suited for vertical-axis wind turbines, which offer stable performance under turbulent and variable wind conditions commonly observed in urban and industrial environments. The integration of a lake water-based multi-effect desalination (MED) subsystem is similarly supported by local environmental conditions. Lake Ontario surface water exhibits relatively low salinity and moderate seasonal temperature variations, typically ranging from near-freezing conditions in winter to approximately 20-25 °C during summer months. These characteristics are favorable for low-temperature thermal desalination processes, as they reduce scaling risk and improve heat transfer performance. Moreover, the availability of a large and stable freshwater source adjacent to the treatment plant enables continuous multi-effect desalination (MED) operation without the need for extensive pretreatment or additional pumping infrastructure.

In addition to site-specific environmental suitability, the integrated system design explicitly accounts for temporal variability in renewable energy supply and waste heat availability. Fluctuations in wind power generation and transient heat recovery from the sludge incineration and hydrochar production units can be mitigated through passive or active thermal energy storage integration. In this context, phase-change-material based thermal storage represents a viable buffering option, particularly within the temperature ranges associated with ORC condenser heat and HTC-driven MED operation. Although phase change material (PCM) storage is not explicitly modeled in the present study, its potential integration could enhance thermal stability, smooth short-term fluctuations, and improve overall system robustness under variable operating conditions. The selection of the Hamilton site and the associated subsystems is strongly supported by local wind characteristics, lake water properties, and opportunities for heat integration and thermal buffering. These location-specific factors reinforce the practical feasibility of the proposed system and highlight its suitability for implementation in municipal wastewater treatment facilities operating under similar environmental conditions.

3. Analysis and assessment

To optimize the energy, water and waste recovery processes in a holistic manner, all sub-components of the system must be examined in detail from a thermodynamic perspective. In this section, the overall performance of the proposed integrated system is evaluated based on mass, energy, and exergy balances. The equations generated for each subsystem aim to demonstrate system efficiency by examining the direct and recovered forms of energy conversion processes. The system design and analysis were conducted considering the Hamilton-Woodward Avenue Wastewater Treatment Plant site in Ontario, Canada. This site was selected because it has a large-scale wastewater treatment infrastructure, generates a high volume of sewage sludge, and offers infrastructure suitable for integration with existing energy recovery systems. Furthermore, because the region is located on the shores of Lake Ontario, it is suitable for the installation of water supply, cooling, and a multi-effect desalination (MED) unit. Hamilton has an active position in renewable energy policies and investments focused on environmental sustainability, increasing the feasibility of an integrated multi-generation system.

To assess the overall performance of the system, mass, energy, entropy, and exergy balances were created for each component and subsystem. These equations were prepared in accordance with the principles of conservation of energy and mass, allowing for a detailed examination of all thermodynamic interactions within the system. In this context, thermodynamic properties at different points in the system were determined, and balance equations were applied for each flow [29]. This analysis is crucial for determining the direction of energy transformations in the system, losses, and recovery potential. The mass, energy, and exergy equations used for each equipment and subsystem are presented in Table 2. In the system solution, mass, energy, and exergy balances for all components were established based on the first and second laws of thermodynamics. In the analysis, the first law provided the principle of energy conservation, while the second law provided the assessment of energy quality and irreversibility [30]. These two fundamental laws were directly applied to the formulation of the balance equations (Table 2) used in all subcomponents of the system.

Using the equations from Table 2, energy inputs, outputs, and exergy losses were calculated for each piece of equipment, and the overall performance parameters of the system (energy and exergy efficiencies) were determined. These equations formed the basis of the holistic thermodynamic analysis of the system. During these analyses, certain assumptions were made to simplify the solution process and ensure consistency in the calculations. These assumptions are presented below.

- Compressor, turbine and pump isentropic efficiencies (η_s): 80%.
- Reference conditions: 298.15 K and 101.3 kPa.
- Negligible pressure losses throughout the current system.
- Adiabatic operation for pumps, compressors and turbines operate under steady-state conditions.
- Sludge lower heating value: 18,000 kJ/kg.
- Specific exergy of sludge: 19,000 kJ/kg.
- Hydrogen specific exergy: 117.12 MJ/kg.
- Specific heat capacity of water: 4.18 kJ/kg.K.
- Hydrogen lower heating value: 120 MJ/kg.
- Hydrochar higher heating value: 26.97 MJ/kg.
- Total annual sludge volume: 22,482 metric tons.
- Organic Rankine cycle (ORC) working fluid: Toluene.

All these assumptions were made to ensure consistency in the thermodynamic analysis of the system and to facilitate the performance evaluation of each subsystem. Based on these assumptions, the entire system was analyzed using the equations in Table 2 using the Aspen Plus, Engineering Equation Solver (EES), and System Advisor Model (SAM) software packages. This allowed for the determination of the thermodynamic properties of each subsystem, detailed evaluation of energy and exergy interactions, and a thermodynamic analysis of the overall system performance.

Table 2
The thermodynamic balance equations written for all system components of the designed system.

Components	Mass Balance	Energy Balance	Entropy Balance	Exergy Balance
Mechanical Dehydrator	$\dot{m}_1 = \dot{m}_2 + \dot{m}_3 + \dot{m}_4$	$\dot{m}_1 h_1 = \dot{m}_2 h_2 + \dot{m}_3 h_3 + \dot{m}_4 h_4$	$\dot{m}_1 s_1 + \dot{S}_{gen,MD} = \dot{m}_2 s_2 + \dot{m}_3 s_3 + \dot{m}_4 s_4$	$\dot{m}_1 ex_1 = \dot{m}_2 ex_2 + \dot{m}_3 ex_3 + \dot{m}_4 ex_4 + \dot{E}x_{Des,MD}$
Dryer	$\dot{m}_3 = \dot{m}_5$	$\dot{m}_3 h_3 + \dot{Q}_{Dryer} = \dot{m}_5 h_5$	$\dot{m}_3 s_3 + \dot{Q}_{Dryer}/T_s + \dot{S}_{gen, Dryer} = \dot{m}_5 s_5$	$\dot{m}_3 ex_3 + \dot{E}x_{Q,Dryer} = \dot{m}_5 ex_5 + \dot{E}x_{Des,Dryer}$
Incinerator	$\dot{m}_2 + \dot{m}_5 = \dot{m}_6$,	$\dot{m}_2 h_2 + \dot{m}_5 h_5 + \dot{S}_{Inc} = \dot{m}_6 h_6$	$\dot{m}_2 s_2 + \dot{m}_5 s_5 + \dot{Q}_{Inc}/T_b + \dot{S}_{gen,Inc} = \dot{m}_6 s_6$	$\dot{m}_2 ex_2 + \dot{m}_5 ex_5 + \dot{E}x_{Q\_Inc} = \dot{m}_6 ex_6 + \dot{E}x_{Des,Inc}$
Evaporator	$\dot{m}_6 = \dot{m}_7$, $\dot{m}_{14} = \dot{m}_{11}$	$\dot{m}_6 h_6 + \dot{m}_{14} h_{14} = \dot{m}_7 h_7 + \dot{m}_{11} h_{11}$	$\dot{m}_6 s_6 + \dot{m}_{14} s_{14} + \dot{S}_{gen,Evap} = \dot{m}_7 s_7 + \dot{m}_{11} s_{11}$	$\dot{m}_6 ex_6 + \dot{m}_{14} ex_{14} = \dot{m}_7 ex_7 + \dot{m}_{11} ex_{11} + \dot{E}x_{Des,Evap}$
Precipitator	$\dot{m}_7 = \dot{m}_8 + \dot{m}_{Ash}$	$\dot{m}_7 h_7 + \dot{W}_{PRC} = \dot{m}_8 h_8 + \dot{m}_{Ash} h_{Ash}$	$\dot{m}_7 s_7 + \dot{S}_{gen,PRC} = \dot{m}_8 s_8 + \dot{m}_{Ash} s_{Ash}$	$\dot{m}_7 ex_7 + \dot{W}_{PRC} = \dot{m}_8 ex_8 + \dot{m}_{Ash} ex_{Ash} + \dot{E}x_{Des,PRC}$
Scrubber	$\dot{m}_8 = \dot{m}_9 + \dot{m}_{Sludge}$	$\dot{m}_8 h_8 + \dot{W}_{SC} = \dot{m}_9 h_9 + \dot{m}_{Sludge} h_{Sludge}$	$\dot{m}_8 s_8 + \dot{S}_{gen,SC} = \dot{m}_9 s_9 + \dot{m}_{Sludge} s_{Sludge}$	$\dot{m}_8 ex_8 + \dot{W}_{SC} = \dot{m}_9 ex_9 + \dot{m}_{Sludge} ex_{Sludge} + \dot{E}x_{Des,SC}$
T-1	$\dot{m}_{11} = \dot{m}_{12}$	$\dot{m}_{11} h_{11} = \dot{m}_{12} h_{12} + \dot{W}_{T-1}$	$\dot{m}_{11} s_{11} + \dot{S}_{gen, T-1} = \dot{m}_{12} s_{12}$	$\dot{m}_{11} ex_{11} = \dot{m}_{12} ex_{12} + \dot{W}_{T-1} + \dot{E}x_{Des, T-1}$
Condenser	$\dot{m}_{12} = \dot{m}_{13}$,	$\dot{m}_{12} h_{12} + = \dot{m}_{13} h_{13} + \dot{Q}_{Out\_Cond}$	$\dot{m}_{12} s_{12} + \dot{S}_{gen, Cond} = \dot{m}_{13} s_{13} + \dot{Q}_{Out\_Cond}/T_b +$	$\dot{m}_{12} ex_{12} = \dot{m}_{13} ex_{13} + \dot{E}x_{Out\_Cond} + \dot{E}x_{Des,Cond}$
P-1	$\dot{m}_{13} = \dot{m}_{14}$	$\dot{m}_{13} h_{13} + \dot{W}_{P-1} = \dot{m}_{14} h_{14}$	$\dot{m}_{13} s_{13} + \dot{S}_{gen,P-1} = \dot{m}_{14} s_{14}$	$\dot{m}_{13} ex_{13} + \dot{W}_{P-1} = \dot{m}_{14} ex_{14} + \dot{E}x_{Des,P-1}$
HE-1	$\dot{m}_4 = \dot{m}_{15}$	$\dot{m}_4 h_4 + \dot{Q}_{In,HE-1} = \dot{m}_{15} h_{15}$	$\dot{m}_4 s_4 + \dot{Q}_{In,HE-1}/T_s + \dot{S}_{gen, HE-1} = \dot{m}_{15} s_{15}$	$\dot{m}_4 ex_4 + \dot{E}x_{Q,In,HE-1} = \dot{m}_{15} ex_{15} + \dot{E}x_{Des,HE-1}$
Dark Fermentation Reactor	$\dot{m}_{15} = \dot{m}_{16} + \dot{m}_{17}$	$\dot{m}_{15} h_{15} = \dot{m}_{16} h_{16} + \dot{m}_{17} h_{17}$	$\dot{m}_{15} s_{15} + \dot{S}_{gen, DF} = \dot{m}_{16} s_{16} + \dot{m}_{17} s_{17}$	$\dot{m}_{15} ex_{15} = \dot{m}_{16} ex_{16} + \dot{m}_{17} ex_{17} + \dot{E}x_{Des, DF}$
Gas Separator	$\dot{m}_{16} = \dot{m}_{18} + \dot{m}_{19}$	$\dot{m}_{16} h_{16} = \dot{m}_{18} h_{18} + \dot{m}_{19} h_{19}$	$\dot{m}_{16} s_{16} + \dot{S}_{gen,DF} = \dot{m}_{18} s_{18} + \dot{m}_{19} s_{19}$	$\dot{m}_{16} ex_{16} = \dot{m}_{18} ex_{18} + \dot{m}_{19} ex_{19} + \dot{E}x_{Des,DF}$
P-2	$\dot{m}_{24} = \dot{m}_{25}$	$\dot{m}_{24} h_{24} + \dot{W}_{P-2} = \dot{m}_{25} h_{25}$	$\dot{m}_{24} s_{24} + \dot{S}_{gen,P-2} = \dot{m}_{25} s_{25}$	$\dot{m}_{24} ex_{24} + \dot{W}_{P-2} = \dot{m}_{25} ex_{25} + \dot{E}x_{Des, P-2}$
P-3	$\dot{m}_{20} = \dot{m}_{21}$	$\dot{m}_{20} h_{20} + \dot{W}_{P-3} = \dot{m}_{21} h_{21}$	$\dot{m}_{20} s_{20} + \dot{S}_{gen, P-3} = \dot{m}_{21} s_{21}$	$\dot{m}_{20} ex_{20} + \dot{W}_{P-3} = \dot{m}_{21} ex_{21} + \dot{E}x_{Des, P-3}$
MED	$\dot{m}_{21} = \dot{m}_{22} + \dot{m}_{23}$	$\dot{m}_{21} h_{21} + \dot{Q}_{In,HE-4} = \dot{m}_{22} h_{22} + \dot{m}_{23} h_{23}$	$\dot{m}_{21} s_{21} + \dot{Q}_{In,HE-4}/T_s + \dot{S}_{gen,Des} = \dot{m}_{22} s_{22} + \dot{m}_{23} s_{23}$	$\dot{m}_{21} ex_{21} + \dot{E}x_{Q\_In,HE-4} = \dot{m}_{22} ex_{22} + \dot{m}_{23} ex_{23} + \dot{E}x_{Des,Des}$
HE-2	$\dot{m}_{25} = \dot{m}_{26}$, $\dot{m}_{28} = \dot{m}_{29}$	$\dot{m}_{25} h_{25} + \dot{m}_{28} h_{28} = \dot{m}_{26} h_{26} + \dot{m}_{29} h_{29}$	$\dot{m}_{25} s_{25} + \dot{m}_{28} s_{28} + \dot{S}_{gen, HE-2} = \dot{m}_{26} s_{26} + \dot{m}_{29} s_{29}$	$\dot{m}_{25} ex_{25} + \dot{m}_{28} ex_{28} = \dot{m}_{26} ex_{26} + \dot{m}_{29} ex_{29} + \dot{E}x_{Des, HE-2}$
HE-3	$\dot{m}_{26} = \dot{m}_{27}$	$\dot{m}_{26} h_{26} + \dot{Q}_{In,HE-3} = \dot{m}_{27} h_{27}$	$\dot{m}_{26} s_{26} + \dot{Q}_{In,HE-3}/T_s + \dot{S}_{gen, HE-3} = \dot{m}_{27} s_{27}$	$\dot{m}_{26} ex_{26} + \dot{E}x_{Q,In,HE-3} = \dot{m}_{27} ex_{27} + \dot{E}x_{Des,HE-3}$
HE-4	$\dot{m}_{31} = \dot{m}_{32}$	$\dot{m}_{31} h_{31} + \dot{Q}_{In,HE-4} = \dot{m}_{32} h_{32}$	$\dot{m}_{31} s_{31} + \dot{Q}_{In,Hex4}/T_s + \dot{S}_{gen, HE-4} = \dot{m}_{32} s_{32}$	$\dot{m}_{31} ex_{31} + \dot{E}x_{Q,In,HE-4} = \dot{m}_{32} ex_{32} + \dot{E}x_{Des, HE-4}$
HE-5	$\dot{m}_{33} = \dot{m}_{34}$	$\dot{m}_{33} h_{33} = \dot{m}_{34} h_{34} + \dot{Q}_{Out,HE-5}$	$\dot{m}_{33} s_{33} + \dot{S}_{gen, Hex5} = \dot{m}_{34} s_{34} + \dot{Q}_{Out,HE-5}/T_s$	$\dot{m}_{33} ex_{33} = \dot{m}_{34} ex_{34} + \dot{E}x_{Q,Out,HE-5} + \dot{E}x_{Des, HE-5}$
HTC Reactors	$\dot{m}_{32} = \dot{m}_{33}$ $\dot{m}_{27} = \dot{m}_{28}$	$\dot{m}_{32} h_{32} + \dot{m}_{33} h_{33} + \dot{Q}_{In\_HTC} = \dot{m}_{27} h_{27} + \dot{m}_{28} h_{28}$	$\dot{m}_{32} s_{32} + \dot{m}_{33} s_{33} + \dot{Q}_{In\_HTC}/T_b + \dot{S}_{gen, HTC} = = \dot{m}_{27} s_{27} + \dot{m}_{28} s_{28}$	$\dot{m}_{32} ex_{32} + \dot{m}_{33} ex_{33} + \dot{E}x_{Q\_In\_HTC} = \dot{m}_{27} ex_{27} + \dot{m}_{28} ex_{28} + \dot{E}x_{Des, HTC}$
Flashing	$\dot{m}_{34} = \dot{m}_{31}$, $\dot{m}_{30} = \dot{m}_{35}$	$\dot{m}_{34} h_{34} + \dot{m}_{30} h_{30} = \dot{m}_{31} h_{31} + \dot{m}_{35} h_{35}$	$\dot{m}_{34} s_{34} + \dot{m}_{30} s_{30} + \dot{S}_{gen,Flash} = \dot{m}_{31} s_{31} + \dot{m}_{35} s_{35}$	$\dot{m}_{34} ex_{34} + \dot{m}_{30} ex_{30} = \dot{m}_{31} ex_{31} + \dot{m}_{35} ex_{35} + \dot{E}x_{Des, Flash}$
Dewatering	$\dot{m}_{20} = \dot{m}_{21}$	$\dot{m}_{20} h_{20} = \dot{m}_{21} h_{21}$	$\dot{m}_{20} s_{20} + \dot{S}_{gen, Dewatering} = \dot{m}_{21} s_{21}$	$\dot{m}_{20} ex_{20} = \dot{m}_{21} ex_{21} + \dot{E}x_{Des, Dewatering}$

3.1. Efficiencies for sludge incineration subsystem

The fundamental thermochemical process in this subsystem occurs when organic compounds in the sludge react with oxygen and undergo a combustion process. The combustion reaction is then generally expressed as follows:

$$C_aH_bO_cN_dS_e + \nu\, O_2 \rightarrow aCO_2 + 2bH_2O + 2dN_2 + eSO_2 + ash \quad (1)$$

The $C_aH_bO_cN_dS_e$represents the average chemical composition of the sludge, while ash refers to the non-combustible inorganic components.

The energy and exergy efficiencies for the specific sludge incineration are calculated as follows:

$$\eta = \frac{\dot{Q}_{out}}{\dot{m}_{sludge} \times \ LHV_{sludge}} \quad (2)$$

and

$$\psi = \frac{\dot{Q}_{out} \ \times \ \left(1 - \frac{T_0}{T_{inc}}\right)}{\dot{m}_{sludge} \times \ \ Ex_{sludge}} \quad (3)$$

3.2. Efficiencies for organic Rankine cycle (ORC) subsystem

The energy and exergy efficiencies for organic Rankine cycle (ORC) are calculated as follows:

$$\eta = \frac{\dot{W}_{net,ORC} + \dot{Q}_{out}}{\dot{Q}_{in,ORC}} \quad (4)$$

and

$$\psi = \frac{\dot{W}_{net,ORC} + \dot{Q}_{out}}{\dot{Ex}^{Q_{in,ORC}}} \quad (5)$$

3.3. Efficiencies for dark fermentation (DF) subsystem

In general, the dark fermentation reaction is represented by glucose, and the most common reaction pathway is called the acetate pathway. This pathway has the highest hydrogen yield. The reaction is expressed as follows:

$$C_6H_{12}O_6 + 2H_2O \rightarrow 2CH_3COOH + 2CO_2 + 4H_2 \quad (6)$$

Alternatively, some microorganisms also produce hydrogen via the butyrate pathway, but at lower efficiency:

$$C_6H_{12}O_6 \rightarrow CH_3CH_2CH_2COOH + 2CO_2 + 2H_2 \quad (7)$$

However, in this study, the acetate pathway reaction was used as the basis for the analysis as it provides maximum hydrogen production.

$$\eta = \frac{\dot{m}_{H_2} \ \times LHV_{H_2}}{\dot{m}_{sludge} \ \times \ \ LHV_{sludge} + \ \ \dot{Q}_{in}} \quad (8)$$

and

$$\psi = \frac{\dot{m}_{H_2} \ \times Ex_{H_2}}{\dot{m}_{sludge} \ \times Ex_{sludge} + \dot{Ex}^{Q_{in}}} \quad (9)$$

3.4. Efficiencies for multi-effect desalination (MED) subsystem

The energy and exergy efficiencies for multi-effect desalination (MED) are calculated as follows:

$$\eta = \frac{\dot{m}_{fw} \times (h_{23} - h_{20})}{\dot{Q}_{in,MED}} \quad (10)$$

and

$$\psi = \frac{\dot{m}_{fw} \times (ex_{23} - ex_{20})}{\dot{Ex}^{Q_{in,MED}}} \tag{11}$$

3.5. Efficiencies for hydrochar production subsystem

To represent the hydrothermal carbonization (HTC) process, we can express the formation of hydrochar reaction follows:

$$C_6H_{12}O_6 \rightarrow C_6H_4O_2\ (\text{Hydrochar}) + 2H_2O + 2CO_2 \tag{12}$$

This reaction demonstrates the basic trend of the hydrothermal carbonization (HTC) process. The C/O ratio increases, water and CO_2 are removed, resulting in a more energy-dense solid fuel.

The energy and exergy efficiencies for hydrochar production subsystem are calculated as follows:

$$\eta = \frac{\dot{m}_{hydrochar} \times LHV_{hydrochar} + \dot{Q}_{net}}{\dot{m}_{sludge} \times LHV_{sludge}} \tag{13}$$

and

$$\psi = \frac{\dot{m}_{hydrochar} \times Ex_{hydrochar} + \dot{Ex}^{Q_{net}}}{\dot{m}_{sludge} \times Ex_{sludge}} \tag{14}$$

3.6. Efficiencies for wind farm subsystem

The wind power calculation for a wind farm is commonly made by

$$P_{Wind} = \frac{1}{2} \times \rho \times A \times V^3 \tag{15}$$

The energy and exergy efficiencies for wind farm are calculated as:

$$\eta = \frac{\dot{W}}{\dot{E}_{in}} \tag{16}$$

and

$$\psi = \frac{\dot{W}}{\dot{Ex}_{in}} \tag{17}$$

3.7. Efficiencies for overall system

The energy and exergy efficiencies for overall system are calculated as follows:

$$\eta = \frac{\dot{m}_{H_2} \times LHV_{H_2} + \dot{m}_{fw} \times (h_{23} - h_{20}) + \dot{m}_{hydrochar} \times LHV_{hydrochar} + \dot{Q}_{out} + \dot{W}_{out}}{\dot{m}_{sludge} \times LHV_{sludge} + \dot{Q}_{in}} \tag{18}$$

and

$$\psi = \frac{\dot{m}_{H_2} \times Ex_{H_2} + \dot{m}_{fw} \times (ex_{23} - ex_{20}) + \dot{m}_{hydrochar} \times Ex_{hydrochar} + \dot{Ex}^{Q_{out}} + \dot{W}_{out}}{\dot{m}_{sludge} \times Ex_{sludge} + \dot{Ex}^{Q_{in}}} \tag{19}$$

3.8. Exergoeconomic and economic feasibility analysis

The total capital investment of the integrated system is calculated as the sum of the capital costs of all major subsystems, including dark fermentation, hydrochar production, organic Rankine cycle (ORC), multi-effect desalination (MED), wind energy, and auxiliary units, as follows:

$$CAPEX_{tot} = \sum_{k=1}^{N} CAPEX_k \tag{20}$$

The total annual operating cost of the integrated system is calculated as:

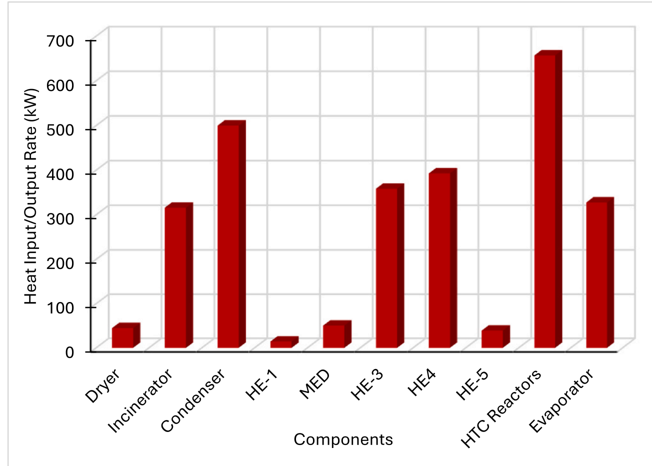

Fig. 2. The heat input and output rates of the system components.

$$OPEX_{tot} = \sum_{k=1}^{N} OPEX_{k,annual} \tag{21}$$

For the dark fermentation (DF) subsystem, the operating cost is expressed as:

$$OPEX_{DF} = C_{nutrient} + C_{separator} + C_{electricity} + C_{maintance} \tag{22}$$

The annual economic benefit of the integrated system is determined by summing revenues obtained from useful products and avoided disposal costs:

$$R_{annual} = R_{H_2} + R_{electricity} + R_{hydrochar} + R_{water} + R_{sludge} \tag{23}$$

The net annual cash flow of the system is calculated as:

$$NCF = R_{annual} - OPEX_{tot} \tag{24}$$

The economic feasibility of the integrated system is evaluated using the simple payback period:

$$SPP = \frac{CAPEX_{tot}}{NCF} \tag{25}$$

As a result of the thermodynamic and exergoeconomic analysis performed in this section, the energy and exergy interactions of all subcomponents of the system were examined in detail and the performance characteristics of each sub-system were determined.

4. Results and discussion

This section presents the key findings of the study, including the thermodynamic performance of the proposed system and its environmental and economic feasibility, providing an integrated assessment of system efficiency, sustainability, and practicality.

4.1. Thermodynamic performance and system outputs

This section presents and discusses the results of the system's thermodynamic analysis. The energy and exergy efficiencies, heat and power distributions, exergy destruction, and production rates are evaluated. Furthermore, the effects of ORC fluid selection and reference temperature on system performance are investigated.

Fig. 2 shows the heat input and output rates in the different components of the system. The results reveal that the HTC reactor has the highest heat demand in the system, at approximately 656.9 kW. This is due to the hydrothermal carbonization (HTC) process occurring at high temperatures (453-473 K) and pressures. The high thermal energy requirement in the reactor is necessary for the organic components within the sludge to decompose and transform into hydrochar, a carbon-rich solid product. The condenser component ranks second with a heat load of approximately 500 kW and transfers a significant portion of the heat released during the condensation of toluene in the ORC cycle to the dark fermentation subsystem. This recovered heat meets the thermal requirements of the sludge in the dark fermentation reactor, enhancing the system's energy integration. The HE-3 and HE-4 heat exchangers, with their respective power outputs of 358.6 kW and 392.9 kW, are the primary intermediate components facilitating the thermal interaction between the sludge incineration, organic Rankine cycle (ORC), and hydrothermal carbonization (HTC) processes. These heat exchangers contribute significantly to overall system efficiency by optimizing energy transfer between the flue gas and process streams.

On the other hand, the evaporator represents the primary evaporation stage of the organic Rankine cycle (ORC) with a heat input of approximately 327.6 kW. In this stage, hot flue gas from the sludge incineration unit vaporizes toluene, creating the energy potential that can be converted into mechanical work in the cycle. Conversely, the lower heat loads on auxiliary equipment such as the dryer (44.6 kW), HE-1 (14.2 kW), and HE-5 (38.9 kW) indicate that these components perform secondary functions in the system. Overall, the obtained results reveal that the most intense heat transfer in the system occurs between the HTC reactor, the ORC condenser, and the incineration unit. This confirms that the integrated structure operates with an effective heat recovery mechanism, energy losses are minimized, and the system exhibits thermodynamically balanced performance.

In the ORC evaporator, high-temperature flue gas enters at approximately 1173 K and is cooled to about 473 K, while the organic working fluid (toluene) is heated to around 418 K at the turbine inlet under a pressure of 1500 kPa. This temperature configuration ensures that the hot stream remains at a higher temperature than the cold stream throughout the heat exchange process, resulting in a minimum approach temperature difference (ΔT_{min}) of approximately 55 K. The pinch point therefore occurs under safe operating conditions without any temperature crossover, confirming that the heat transfer process respects practical heat transfer constraints. The minimum approach temperature analysis provides an equivalent validation of heat exchanger feasibility. Consequently, the heat duties reported in Fig. 2 are thermodynamically sound and physically realistic within the defined system boundaries accordingly.

Fig. 3 shows the power input/output ratios of the turbines and pumps in the system. Turbine (T-1) has the highest power output at approximately 99 kW and is the main source of mechanical work in the organic Rankine cycle (ORC). The turbine's high-power output demonstrates that the evaporation and expansion processes of the organic fluid are efficient. Pumps (P-1, P-2, and P-3) provide fluid circulation in the system with power consumptions of 15 kW, 3.3 kW, and 2.3 kW, respectively. Since the total energy consumption of the pumps constitutes a relatively small portion of the power generated by the turbine, net power production throughout the system is positive. This demonstrates that the organic Rankine cycle (ORC) is effective in terms of energy recovery and that mechanical losses are low.

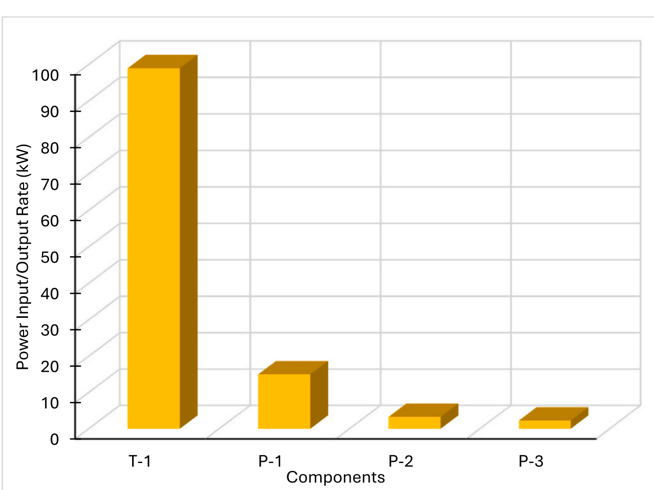

Fig. 3. The power input and output rates of the system components.

The distribution of entropy generation (S_{gen}) within the system serves as an important indicator for assessing the degree of irreversibility and, consequently, the exergy losses associated with each component. For each component, the S_{gen} ratio was calculated by dividing its individual entropy generation value by the total entropy generation of the system (total $S_{gen} = 3.05$ kJ/K). As shown in Fig. 4, the HE-2, HE-3, evaporator, and condenser components account for most of the total entropy generation in the system. This result indicates that heat transfer processes occurring in these components, characterized by large temperature differences, are the primary sources of entropy generation.

The highest S_{gen} ratios are observed in HE-2 (0.834) and HE-3 (0.697), suggesting that optimizing the temperature gradients and flow direction within these heat exchangers is essential to minimize energy losses. Similarly, the evaporator (0.534) and condenser (0.290) also exhibit significant entropy generation, indicating that the efficiency of heat recovery processes in these components limits overall system performance. Lower entropy generation ratios were observed in pumps (P-1, P-2, P-3), flashing, HTC reactor, dark fermentation reactor (DFR), and dryer, as these components operate with lower temperature gradients or lower flow energy, thus contributing less to total entropy generation.

Overall, the results show that the major exergy destruction occurs in the heat exchangers and thermal cycle components. Therefore, by improving the heat transfer surface area, reducing temperature differences, and optimizing flow configuration, total system entropy generation can be reduced. As a result, the exergy efficiency and thermodynamic performance of the entire integrated system can be significantly enhanced.

Fig. 5 shows the exergy destruction rates for the system components. The highest exergy losses were observed in units HE-2 (248.5 kW), HE-3 (207.9 kW), and evaporator (159.2 kW). The high exergy destruction observed in HE-2 and HE-3 is mainly caused by large temperature differences combined with high mass flow rates during heat transfer. In HE-2, hot slurry leaving the hydrothermal carbonization unit at approximately 453-473 K transfers heat to incoming sludge at near-ambient temperature (~298 K), resulting in a temperature difference exceeding 150 K and significant entropy generation. Similarly, HE-3 operates by transferring heat from a high-temperature stream (above 450 K) to a colder process stream in the range of 300-320 K, again under substantial mass flow conditions. From a heat-transfer perspective, these conditions correspond to steep temperature gradients in a conceptual temperature-heat profile, which explains the exergy destruction rates exceeding 200 kW in both units.

The condenser (86.6 kW) and HE-4 (57.6 kW) also produced significant losses, accounting for approximately half of the total exergy destruction. In contrast, components such as pumps, turbines, flashing units, and the HTC reactor operate with smaller temperature differences (<10 kW) and therefore exhibit much lower irreversibilities. The results indicate that the dominant exergy losses in the system originate from heat exchangers handling large thermal duties under pronounced temperature mismatches, emphasizing the importance of heat-transfer optimization to improve system exergy efficiency.

Fig. 6 illustrates the variation of overall exergy efficiency with increasing reference temperature for different ORC working fluids. As the reference temperature increases, a consistent decrease in exergy efficiency is observed for all fluids due to the reduction in available useful energy. Among the investigated fluids, cyclohexane exhibits the highest exergy efficiency (45-41%), followed closely by toluene (44-40%), while 1,1,1,3,3-pentafluoropropane (R245fa) shows the lowest

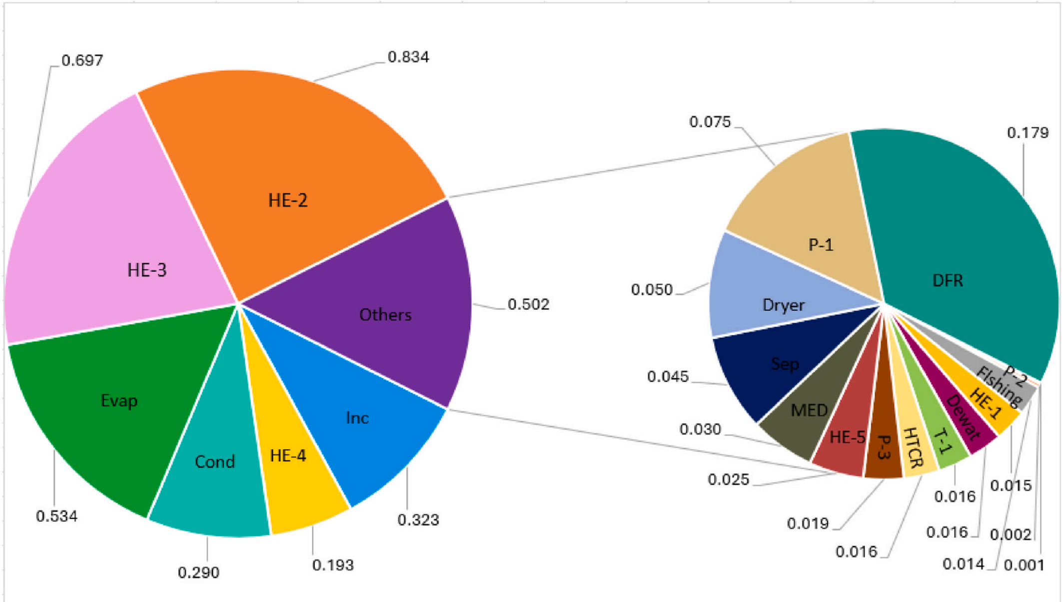

Fig. 4. The entropy generation ratios determined for the system components.

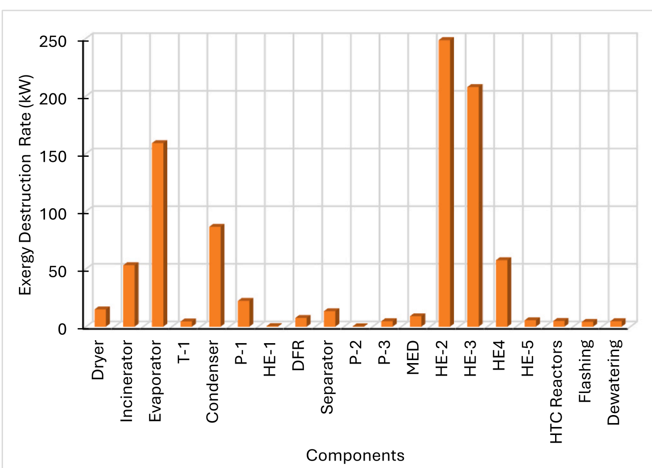

Fig. 5. The exergy destruction rates of the system components.

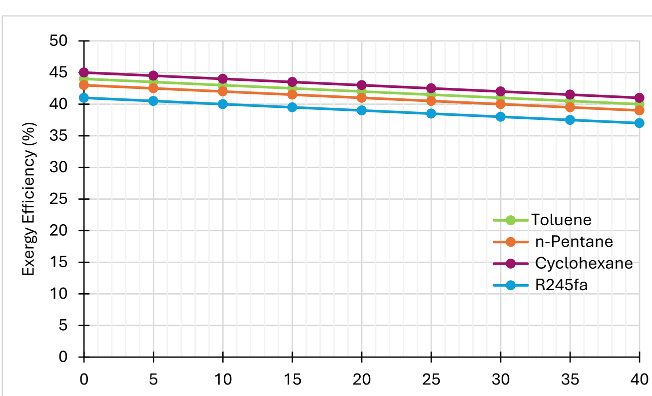

Fig. 6. Variations of overall exergy efficiencies with the reference temperature for various ORC working fluids.

performance, which can be attributed to its relatively low critical temperature.

Although cyclohexane slightly outperforms Toluene in terms of exergy efficiency, the selection of an ORC working fluid for a sustainable integrated system cannot be based on thermodynamic performance alone. Therefore, the working fluid selection was further evaluated by qualitatively considering environmental, safety, and economic aspects. Compared to commonly used refrigerants such as R245fa, which are reported in the literature to have high global warming potential, aromatic hydrocarbons such as toluene are generally associated with negligible ozone depletion potential. Siloxane-based fluids, while suitable for high-temperature organic Rankine cycle (ORC) applications, are often associated with higher cost and limited availability, which can affect large-scale deployment.

From a safety perspective, hydrocarbons are flammable; however, toluene operates at moderate pressures and has a long history of industrial use, with established handling and safety practices. In addition, toluene offers high thermal stability over a wide temperature range relevant to the proposed system, supporting reliable long-term operation. Its wide availability and relatively low cost further contribute to its practical suitability. Considering the combined thermodynamic trends shown in Fig. 6 and the qualitative assessment of environmental impact, safety, and cost, toluene is identified as the most balanced ORC working fluid for the proposed integrated system. This selection supports both efficient energy recovery and practical implementation while remaining consistent with sustainability considerations.

Fig. 7 shows the monthly changes in the amounts of hydrogen, hydrocarbons (hydrochar), and freshwater produced by the system throughout the year. Production values were determined based on thermodynamic analysis and energy balance calculations. According to the results, hydrogen production reaches a maximum in the summer months (July-August), reaching around 1300 kg/month, and decreases to approximately 1000 kg/month in the winter months. This change is associated with increased dark fermentation (DF) efficiency and increased biochemical reaction rates with increasing temperature.

Fig. 8 shows wind speed and the corresponding wind turbine power generation throughout the year. The data was analyzed using the System Advisor Model (SAM) based on typical meteorological conditions for the Ontario region. The wind speeds range from 2 to 22 m/s throughout the year, and power generation fluctuates between 0 and 50 kW. This fluctuation is due to seasonal atmospheric changes, temperature

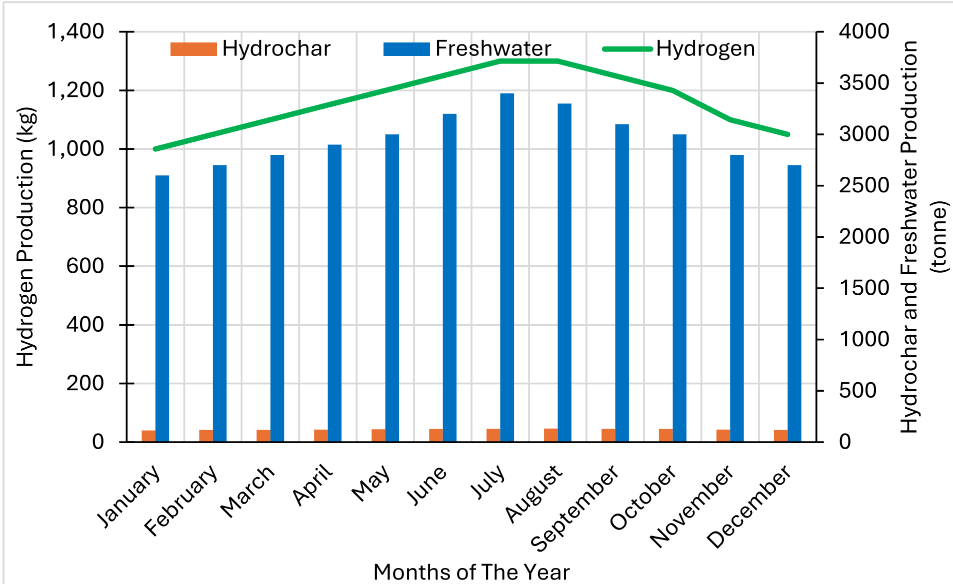

Fig. 7. The monthly variations of hydrogen, hydrochar, and freshwater production throughout the year.

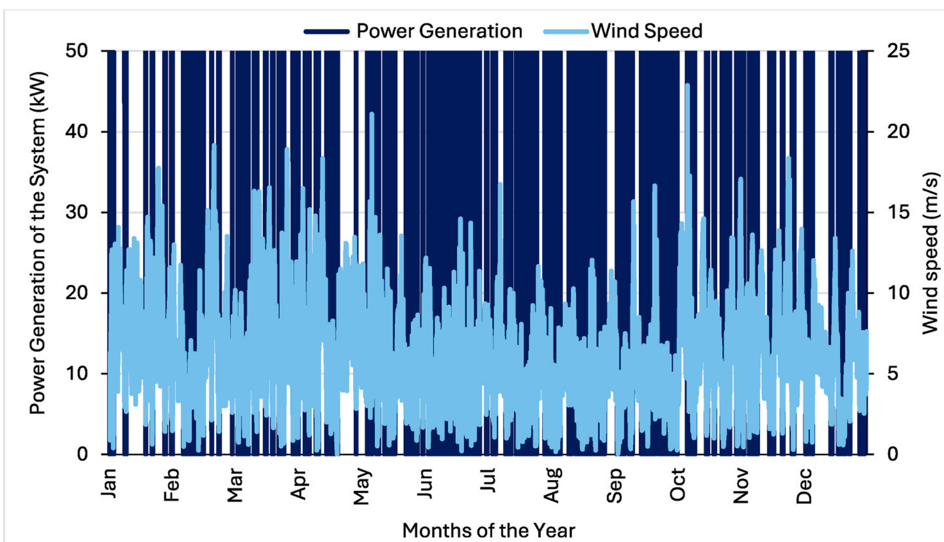

Fig. 8. The hourly wind speed and corresponding power generation of the wind farm over one year.

gradients, pressure differences, and local turbulence. Wind speeds increase particularly in the spring (March-May) and autumn (September-November), maximizing the system's power generation capacity. In the summer, a decrease in power generation is observed due to decreasing wind intensity. This variation reflects the wind farm's natural intermittent power generation characteristics. However, thermal and electrical integration with other system components (especially organic Rankine cycle (ORC), multi-effect desalination (MED), and dark fermentation (DF)) mitigates the negative impact of this variability on overall system performance. As a result, the wind farm is the mainstay of the system's carbon-neutral energy production and significantly contributes to the system's sustainability and energy security goals by providing continuous power support from renewable sources.

The subsystems of the proposed integrated system operate in a coordinated manner through an integrated operational strategy. The short-term fluctuations arising from intermittent power sources, such as wind or from variable biological process, such as dark fermentation, are mitigated through intermediate buffering and process decoupling. In particular, the organic Rankine cycle (ORC) and multi-effect desalination (MED) units are primarily driven by relatively stable waste heat streams from the incineration process, which are less sensitive to upstream variability. This thermal decoupling allows continuous and stable heat integration for the organic Rankine cycle (ORC) and multi-effect desalination (MED) units, while upstream fluctuations are absorbed without compromising overall system efficiency.

Fig. 9 shows the energy and exergy efficiencies of all subcomponents and the overall system. According to the results, the highest energy efficiency, 60%, was achieved in the sludge incineration subsystem. This is due to the high energy conversion potential of the combustion process, which occurs at high temperatures. In contrast, the highest exergy efficiency was observed in the organic Rankine cycle (ORC) subsystem, at 55%. The ORC system was the most efficient cycle in terms of exergy because it enabled the efficient conversion of waste heat into electrical energy. The dark fermentation (DF) process, on the other hand, had the lowest energy efficiency (10%) due to biological reaction limitations and low reaction temperatures. However, when evaluated in terms of

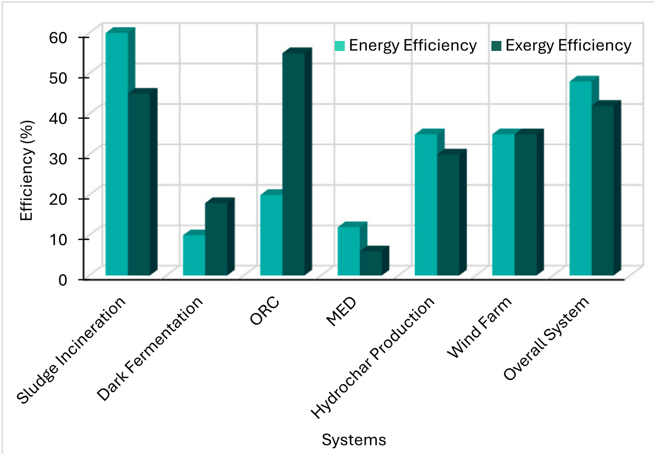

Fig. 9. Comparison of energy and exergy efficiencies for the overall system and its subsystems.

chemical conversion, the exergy efficiency increased to 18%. Because the multi-effect desalination (MED) unit operates on low-temperature heat sources, its energy (12%) and exergy (6%) efficiencies are relatively low. Nevertheless, it contributes to the overall sustainability of the system in terms of waste heat utilization.

The hydrochar production and wind farm subsystems demonstrated stable performance within the range of 35% energy and 30-35% exergy efficiencies range, respectively. These two subsystems supported the system's multigeneration capacity in terms of both thermochemical conversion and renewable electricity generation. The overall system's energy and exergy efficiencies were determined to be 48% and 42%, respectively. These values demonstrate that the multigeneration approach offers a thermodynamically balanced and sustainable structure, minimizing losses through the integration of different energy types.

The validity of the adopted modeling assumptions was evaluated through comparison with representative values reported in the literature. The wastewater sludge composition considered in this study, with a volatile solid (VS) content typically in the range of 60-75% of total solids and a high moisture content, is consistent with reported characteristics of municipal sewage sludge [29]. The hydrothermal carbonization (HTC) process was modeled at 220-250 °C and 2-3 MPa, yielding a hydrochar mass fraction of approximately 55-60% on a dry basis, which agrees well with experimental HTC studies on sewage sludge reporting hydrochar yields in the range of 50-65% [23]. For the dark fermentation (DF) subsystem, hydrogen production was assumed to occur under mesophilic conditions (∼37 °C), with hydrogen yields within 80-120 L H_2 kg^{-1} VS, matching the range commonly reported for sludge-based dark fermentation systems [31]. The wind farm electricity generation was simulated using the system advisor model (SAM), and the predicted annual power output per installed capacity is consistent with reported performance of small-scale wind turbines operating under similar wind speed conditions [32]. These comparisons demonstrate that the selected input parameters and resulting performance indicators fall within well-established experimental and modeling ranges, thereby supporting the credibility and realism of the proposed integrated system analysis.

Fig. 10 presents a scenario-based sensitivity analysis focusing on the multi-effect desalination (MED) and dark fermentation (DF) subsystems, which exhibit the lowest exergy efficiencies in the integrated system. The base case indicates that dark fermentation (DF) is the dominant contributor to subsystem-level exergy destruction, while multi-effect desalination (MED) also introduces notable irreversibilities associated with low-temperature heat utilization. Improving the multi-effect desalination (MED) subsystem through enhanced heat integration results in a moderate reduction in both local and overall exergy destruction. In contrast, improvements in the dark fermentation process, primarily associated with increased hydrogen yield and reduced process losses, lead to a more significant decrease in total system exergy destruction. The combined improvement scenario achieves the lowest overall exergy destruction, highlighting the synergistic impact of simultaneously enhancing thermal and biochemical subsystems. These results demonstrate that targeted improvements in low-efficiency components can effectively enhance the overall exergy performance of the integrated system.

4.2. Exergoeconomic assessment and economic feasibility

The exergoeconomic assessment demonstrates that the proposed integrated wastewater sludge management system provides meaningful economic advantages through resource recovery and waste valorization. As summarized in Table 3, the system combines multiple outputs within

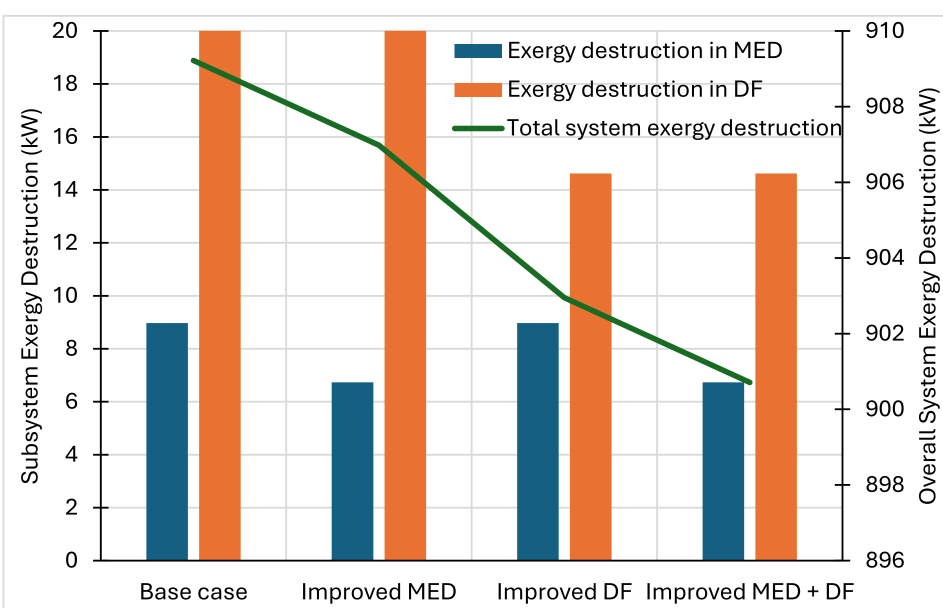

Fig. 10. The sensitivity analysis results of the exergy destruction in the MED and DF subsystems and the resulting impact on total system exergy destruction under different improvement scenarios.

Table 3
Summary of exergoeconomic and economic feasibility indicators for the designed system.

Category	Parameter	Value
Capital investment	$CAPEX_{tot}$	16.6 million USD
	Dominant CAPEX contributor	Dark fermentation subsystem
Operating cost	$OPEX_{tot}$	1.80×10^5 USD/year
	Dark fermentation OPEX	4.46×10^4 USD/year
	Main dark fermentation (DF) cost drivers	Nutrients and gas separation
Economic benefits	Annual revenue (R)	6.09×10^5 USD/year
	Dominant benefit	Sludge disposal avoidance
Overall feasibility	Net annual cash flow (NCF)	4.29×10^5 USD/year
	Simple payback period (SPP)	38.7 years

a single integrated configuration, enabling diversified economic benefits rather than reliance on a single revenue stream.

A key positive outcome of the analysis is the significant contribution of avoided sludge disposal costs to the overall economic performance. By converting wastewater sludge into valuable products, the system reduces the need for conventional disposal pathways, which represents a major economic burden for municipal wastewater treatment plants. This avoided cost emerges as the dominant economic driver, highlighting the strong alignment of the proposed system with circular economy and sustainable waste management principles.

The integration of thermochemical, biochemical, and renewable energy-based subsystems further enhances economic performance by minimizing external energy requirements. In particular, the use of waste heat recovered from the ORC condenser to supply the thermal demand of the dark fermentation (DF) unit eliminates the need for external heat input, reducing operating costs and improving overall system efficiency. Similarly, the utilization of low-grade heat from the hydrochar production process to drive the multi-effect desalination (MED) subsystem enables freshwater production with minimal additional energy expenditure.

Although the dark fermentation (DF) subsystem constitutes a major share of both capital investment and operating costs, its integration within the broader system framework allows its economic impact to be partially offset through shared infrastructure, energy integration, and downstream product recovery. This integrated design approach distinguishes the proposed system from standalone biohydrogen production units and improves its overall economic robustness.

The system achieves a positive net annual cash flow, confirming its economic viability from a long-term infrastructure perspective. While the simple payback period remains relatively long, this result reflects the capital-intensive nature of advanced municipal waste-to-energy systems rather than a fundamental limitation of the proposed design. The findings indicate that the economic feasibility of the system is primarily driven by waste management benefits, process integration, and resource recovery, underscoring its potential as a sustainable and multifunctional solution for wastewater treatment facilities.

4.3. Environmental performance and carbon management of the designed system

The environmental performance of the proposed integrated system is determined by the management of carbon flows and by-products within the defined system boundary, in addition to its energy performance. Accordingly, the low-carbon and circular characteristics of the system are evaluated by explicitly tracking carbon pathways associated with hydrochar, secondary ash from incineration, and carbon dioxide generated across biological and thermochemical processes.

Hydrochar is considered a carbon-rich intermediate with defined long-term utilization and sequestration pathways, enabling partial retention of biogenic carbon outside the atmosphere. The secondary ash produced during incineration is managed through controlled reuse options or stabilized disposal, preventing the transfer of environmental burdens beyond the system boundary. Carbon dioxide streams originating from both dark fermentation and incineration flue gas are explicitly included in the assessment and addressed through defined long-term management and utilization options consistent with large-scale operation.

A system-level carbon balance is therefore constructed by quantifying carbon input from the biomass feedstock and distributing it among solid carbon retained in hydrochar, carbon associated with ash, and carbon released as CO_2 through biological conversion and incineration. This explicit accounting of all major carbon pathways within the system boundary demonstrates that the low-carbon and circular claims of the proposed system are supported by transparent carbon management rather than qualitative assumptions.

In summary, the results demonstrate the system's high efficiency and sustainability potential in terms of energy recovery, waste management, and multi-product generation. This integrated structure reduces environmental impact by enabling the efficient use of different energy types and provides a strong example of integrated renewable energy solutions.

5. Conclusions

In this study, a sustainable multigeneration system integrating sludge incineration, dark fermentation (DF), hydrochar production with hydrothermal carbonization (HTC), organic Rankine cycle (ORC), multi-effect desalination (MED), and wind farm subsystems were thermodynamically analyzed. The system aims to increase energy recovery and resource efficiency by combining electricity, hydrogen, hydrochar, and freshwater production within the same structure.

The analysis results revealed an overall energy efficiency of 48% and an exergy efficiency of 42%. The highest energy efficiency was achieved in the sludge incineration unit, at 60%, due to the high conversion of chemical energy to thermal energy during the incineration process. The organic Rankine cycle (ORC) subsystem, with an exergy efficiency of 55%, was the most efficient cycle in the system, enabling the efficient conversion of waste heat to electrical energy. While the efficiencies in the dark fermentation (DF) and multi-effect desalination (MED) subsystems are relatively low, it contributes significantly to the sustainability of the system through hydrogen and freshwater production.

The parametric analysis demonstrated that toluene is the most suitable working fluid for the organic Rankine cycle (ORC). Toluene, thanks to its high thermal stability and favorable evaporation temperature, exhibited the most consistent performance, maintaining exergy efficiency values of 40-44% in the 0-40 °C range. According to annual production results, the system produces approximately 13.95 tons of hydrogen, 1490 tons of hydrochar, and 35,500 m^3 of freshwater. Furthermore, the wind farm provides stable electricity generation despite fluctuating wind speeds throughout the year, meeting the system's energy requirements from renewable sources.

Overall, the proposed system has high potential for converting waste into energy and valuable products, making a significant contribution to the goals of energy efficiency, environmental sustainability, and resource circularity. The results demonstrate that the system is a viable model for industrial-scale wastewater treatment plants and constitutes a strong example for integrated renewable energy-based solutions within the framework of circular economy principles.

CRediT authorship contribution statement

Ayse Sinem Meke: Writing – original draft, Validation, Software, Methodology, Investigation, Formal analysis, Data curation. **Ibrahim Dincer:** Writing – review & editing, Supervision, Resources, Project administration, Funding acquisition, Conceptualization. **Ali Khalvati:** Writing – review & editing, Funding acquisition.

Declaration of competing interest

The authors declare that they have no known competing financial interests or personal relationships that could have appeared to influence the work reported in this paper.

Nomenclature

A	area (m^2)
C	cost (USD)
E	total energy (kJ)
$\dot{E}$	energy rate (kW)
ex	specific exergy (kJ/kg)
$\dot{E}x$	exergy rate (kW)
$\dot{E}x_d$	exergy rate (kW)
$\dot{E}x_Q$	exergy transfer associated with heat transfer (kJ)
h	specific enthalpy (kJ/kg)
H	enthalpy (kJ)
HHV	higher heating value (kJ/kg)
LHV	lower heating value (kJ/kg)
m	mass (kg)
M	molar mass (kg/kmol)
$\dot{m}$	mass flow rate (kg/s)
N	project lifetime (years)
Q	heat transfer (kJ)
$\dot{Q}$	heat transfer rate (kW)
Q_H	heat transfer rate with high temperature source (kJ)
Q_L	heat transfer rate with low temperature sink (kJ)
R	revenue (USD/year)
s	specific entropy (kJ/kg.K)
ρ	density (kg/m^3)
S	entropy (kJ/K)
$\dot{S}$	entropy rate (kW)
T	temperature (K)
V	speed (m/s)
w	specific work (kJ/kg)
W	total work (kJ)
$\dot{W}$	work rate or power (kW)

Subscripts

0	reference points
1,2,3 …	state points
f	final
gen	generation
i	initial
in	inlet
k	component
out	outlet
tot	total

Greek Letters

η	energy efficiency
ψ	exergy efficiency

Abbreviations

BGFT	biogas-fueled gas turbine
C	compressor
CAPEX	capital expenditure
CSP	concentrated solar power
DF	dark fermentation
EBE	energy balance equations
EES	engineering equation solver
EnBE	entropy balance equations
ExBE	exergy balance equations
Gen	generator

GHG	greenhouse gas
HE	heat exchanger
HTC	hydrothermal carbonization
HTF	heat transfer fluid
HYSYS	hyprotech systems
MBE	mass balance equations
MED	multi effect desalination
NCF	net annual cash flow
OPEX	operational expenditure
ORC	organic Rankine cycle
P	pump
PCM	phase change material
PEM	proton exchange membrane
PTC	parabolic trough collector
R	reactor
RO	reverse osmosis
S	separator
SAM	system advisor model
SPP	simple payback period
SSE	single-stage evaporation
T	turbine
TES	thermal energy storage
Val	valve
VS	volatile solid
WWTP	wastewater treatment plant

Data availability

Some of the data may be made available on request.

References

[1] Bhol S, Sahu NC. Optimal scheduling of renewable sources based micro grid with PV and battery storage using crayfish optimization algorithm. Energy Storage 2024;6(6):e70027. https://doi.org/10.1002/est2.70027.

[2] Rigolon A, Tabassum N, Ewing R. Climate adaptation strategies for active transportation: barriers and facilitators in US cities. Sustain Cities Soc 2024;117:105956. https://doi.org/10.1016/j.scs.2024.105956.

[3] Fetanat A, Tayebi M, Mofid H. Water-energy-carbon nexus and sustainability-oriented prioritization of negative emissions technologies for the oil & gas industry: a decision support system under fermatean fuzzy environment. Process Saf Environ Prot 2023;179:462–83. https://doi.org/10.1016/j.psep.2023.09.037.

[4] Zuo L, Ren Y. How renewable energy consumption and digitalization contribute to environmental sustainability: evidence from one belt one road countries. J Environ Manag 2025;380:124379. https://doi.org/10.1016/j.jenvman.2025.124379.

[5] Aridi R, Aridi M, Pannier ML, Lemenand T. Eco-environmental, and social impacts of producing electricity with various renewable energy sources. Energy 2025;320:135139. https://doi.org/10.1016/j.energy.2025.135139.

[6] Horpynko YI, Senetskyi OV. Activation of absorption chillers by the transit heat flow of the energy cycle in cogeneration solar systems. Therm Sci Eng Prog 2023;43:101947. https://doi.org/10.1016/j.tsep.2023.101947.

[7] Ceglia F, Marrasso E, Roselli C, Sasso M. Energy and environmental assessment of a biomass-based renewable energy community including photovoltaic and hydroelectric systems. Energy 2023;282:128348. https://doi.org/10.1016/j.energy.2023.128348.

[8] Taroual K, Nachtane M, Adeli K, Faik A, Boulzehar A, Saifaoui D, Tarfaoui M. Hybrid marine energy and AI-driven optimization for hydrogen production in coastal regions. Int J Hydrogen Energy 2025;118:80–92. https://doi.org/10.1016/j.ijhydene.2025.03.091.

[9] Ghanavati F, Matias JC, Osório GJ. Towards sustainable smart cities: integration of home energy management system for efficient energy utilization. Sustain Cities Soc 2024;111:105579. https://doi.org/10.1016/j.scs.2024.105579.

[10] Lucas M, Komesse HB, Duval—Dachary S, Teixeira D. Comparative environmental impact assessment of a daily electricity restitution operated by advanced adiabatic compressed air energy storage systems (A-CAES). Energy Storage 2025;7(4):e70194. https://doi.org/10.1002/est2.70194.

[11] Flórez-Orrego D, Dardor D, Germanier R, Margni M, Maréchal F. A systemic study for decarbonizing secondary aluminium production via waste heat recovery, carbon management and renewable energy integration. Energy Convers Manag 2025;341:120021. https://doi.org/10.1016/j.enconman.2025.120021.

[12] Temiz M, Dincer I. Cleaner production of energy and fuels from a renewable energy-based self-sufficient system with energy storage options. J Energy Storage 2023;72:108415. https://doi.org/10.1016/j.est.2023.108415.

[13] Scherer, J., Wolfersdorf, C., Ginsberg, T., & Richter, A. A study of the phosphorus release potential of sewage sludge in entrained flow gasification. Available at: SSRN 5049143. https://doi.org/10.1016/j.fuel.2025.136975.

[14] Morrison M, Srinivasan RS, Ries R. Complementary life cycle assessment of wastewater treatment plants: an integrated approach to comprehensive upstream and downstream impact assessments and its extension to building-level wastewater generation. Sustain Cities Soc 2016;23:37–49. https://doi.org/10.1016/j.scs.2016.02.013.

[15] Huang C, Mohamed BA, Li LY. Comparative life-cycle energy and environmental analysis of sewage sludge and biomass co-pyrolysis for biofuel and biochar production. Chem Eng J 2023;457:141284. https://doi.org/10.1016/j.cej.2023.141284.

[16] Yaphary YL, Wee JX, Li SFY. Synergistic resource recoveries of phosphorus and useable water from sewage sludge incineration ash and concrete slurry wastewater. Resour Conserv Recycl 2025;212:107956. https://doi.org/10.1016/j.resconrec.2024.107956.

[17] Ebrahimi A, Houshfar E. Thermodynamic analysis and optimization of the integrated system of pyrolysis and anaerobic digestion. Process Saf Environ Prot 2022;164:582–94. https://doi.org/10.1016/j.psep.2022.06.043.

[18] Teymouri M, Shokravi Z, Moghimi H. Dark fermentation for biohydrogen and bioethanol production. In: Transformation of liquid waste to energy. Woodhead Publishing; 2026. p. 291–318. https://doi.org/10.1016/B978-0-443-33683-6.00003-6.

[19] Akbari S, Farahani MF, Hosseinzadeh K. Theoretical analysis of transient counter-flow combustion system fueled by porous biomass particles in a non-premixed configuration under non-adiabatic conditions. Int J Thermofluids 2024;22:100653. https://doi.org/10.1016/j.ijft.2024.100653.

[20] Goren AY, Dincer I, Khalvati A. Development of a unique integrated bioreactor for simultaneous desalination and bioenergy and biohydrogen production. Chem Eng J 2024;486:150312. https://doi.org/10.1016/j.cej.2024.150312.

[21] Sillero L, Solera R, Perez M. Biochemical assays of potential methane to test biogas production from dark fermentation of sewage sludge and agricultural residues. Int J Hydrogen Energy 2022;47(27):13289–99. https://doi.org/10.1016/j.ijhydene.2022.02.080.

[22] Zin MMT, Tiwari D, Kim DJ. Recovery of ammonium and phosphate as struvite via integrated hydrolysis and incineration of sewage sludge. J Water Proc Eng 2021;39:101697. https://doi.org/10.1016/j.jwpe.2020.101697.

[23] Gao X, Chen H, Zheng H, Zhang Y, Wei L, Pan P. Performance assessment of a multiple generation system integrating sludge hydrothermal treatment with a small modular nuclear reactor power plant. Energy 2025;315:134323. https://doi.org/10.1016/j.energy.2024.134323.

[24] Aydin MI, Karaca AE, Qureshy AM, Dincer I. A comparative review on clean hydrogen production from wastewaters. J Environ Manag 2021;279:111793. https://doi.org/10.1016/j.jenvman.2020.111793.

[25] Guan M, Wang J, Jin H, Wei W. Thermochemical conversion and gasification of high-density polyethylene (HDPE) in supercritical CO2: a sustainable approach to plastic waste management. Chem Eng J 2025;512:162343. https://doi.org/10.1016/j.cej.2025.162343.

[26] Fatigati F, Cipollone R. Experimental and theoretical assessment of the effects of electrical load variation on the operability of a small-scale Organic Rankine Cycle

(ORC)-based unit equipped with a hermetic scroll expander. Energy 2024;311: 133318. https://doi.org/10.1016/j.energy.2024.133318.
[27] Teng S, Li L, Yan C, An D, Zhao Y, Xi H. Multi-parameter experimental study of a tesla turbine applied to an organic Rankine cycle system for low-grade heat utilisation. Energy Convers Manag 2025;333:119824. https://doi.org/10.1016/j.enconman.2025.119824.
[28] Abdolalipouradl M, Mohammadkhani F, Yari M. The potential of a novel multigeneration system based on a biogas-fueled gas turbine: thermodynamic, exergoeconomic, and multi-objective assessments. Renew Energy 2025:123282. https://doi.org/10.1016/j.renene.2025.123282.
[29] Liu H, Basar IA, Eskicioglu C. Effects of municipal sludge composition on hydrothermal liquefaction products: optimizing energy recovery via combination with anaerobic digestion. Chem Eng J 2025:170645. https://doi.org/10.1016/j.cej.2025.170645.
[30] Dincer I. Thermodynamics: a smart approach. John Wiley & Sons; 2020.
[31] Lim SW, Nandong J. Modeling of biohydrogen production using generalized multi-scale kinetic model: impacts of fermentation conditions. Int J Hydrogen Energy 2022;47(41):17926–45. https://doi.org/10.1016/j.ijhydene.2022.03.291.
[32] Testi A, de Souza TM, de Barros Trannin IC. Technical and economic feasibility of a small vertical axis wind turbine in low wind conditions compared to other power sources for pumping water. J Clean Prod 2024;470:143328. https://doi.org/10.1016/j.jclepro.2024.143328.